

Spatial vision in the purple sea urchin *Strongylocentrotus purpuratus* (Echinoidea)

D. Yerramilli and S. Johnsen*

Biology Department, Duke University, Durham, NC 27708, USA

*Author for correspondence (sjohnsen@duke.edu)

Accepted 14 October 2009

SUMMARY

Recent evidence that echinoids of the genus *Echinometra* have moderate visual acuity that appears to be mediated by their spines screening off-axis light suggests that the urchin *Strongylocentrotus purpuratus*, with its higher spine density, may have even more acute spatial vision. We analyzed the movements of 39 specimens of *S. purpuratus* after they were placed in the center of a featureless tank containing a round, black target that had an angular diameter of 6.5 deg. or 10 deg. (solid angles of 0.01 sr and 0.024 sr, respectively). An average orientation vector for each urchin was determined by testing the animal four times, with the target placed successively at bearings of 0 deg., 90 deg., 180 deg. and 270 deg. (relative to magnetic east). The urchins showed no significant unimodal or axial orientation relative to any non-target feature of the environment or relative to the changing position of the 6.5 deg. target. However, the urchins were strongly axially oriented relative to the changing position of the 10 deg. target (mean axis from -1 to 179 deg.; 95% confidence interval ± 12 deg.; $P < 0.001$, Moore's non-parametric Hotelling's test), with 10 of the 20 urchins tested against that target choosing an average bearing within 10 deg. of either the target center or its opposite direction (two would be expected by chance). In addition, the average length of the 20 target-normalized bearings for the 10 deg. target (each the vector sum of the bearings for the four trials) were far higher than would be expected by chance ($P < 10^{-10}$; Monte Carlo simulation), showing that each urchin, whether it moved towards or away from the target, did so with high consistency. These results strongly suggest that *S. purpuratus* detected the 10 deg. target, responding either by approaching it or fleeing it. Given that the urchins did not appear to respond to the 6.5 deg. target, it is likely that the 10 deg. target was close to the minimum detectable size for this species. Interestingly, measurements of the spine density of the regions of the test that faced horizontally predicted a similar visual resolution (8.3 ± 0.5 deg. for the interambulacrum and 11 ± 0.54 deg. for the ambulacrum). The function of this relatively low, but functional, acuity – on par with that of the chambered *Nautilus* and the horseshoe crab – is unclear but, given the bimodal response, is likely to be related to both shelter seeking and predator avoidance.

Key words: diffuse sensory system, echinoid, marine ecology, spatial vision, vision.

INTRODUCTION

Echinoderm photoreception is a well-studied but puzzling phenomenon. Light-mediated behaviors are ubiquitous in this phylum, including simple phototaxis, covering reactions, UV avoidance, homing, polarization sensitivity, color changes, shelter seeking, diurnal migrations and movement towards small dark objects (Millot, 1954; Millot, 1955; Thornton, 1956; Yoshida, 1966; Millot and Yoshida, 1960; Scheibling, 1980; Hendler, 1984; Johnsen, 1994; Johnsen and Kier, 1999; Adams, 2001; Blevins and Johnsen, 2004). However, the underlying architecture and abilities of this system have remained mysterious.

With the exception of the ocelli found at the tips of the arms of certain asteroids and the tentacular nerves of the holothurian *Opheodesoma spectabilis*, echinoderms have no discrete visual organs (reviewed by Yoshida et al., 1983). Instead, neurological and behavioral evidence suggests that their photosensitivity is diffuse and located above, below and even within the calcitic endoskeleton (Yoshida, 1979; Moore and Cobb, 1985; Aizenberg, 2001). More recently, Burke et al. (Burke et al., 2006) and Raible et al. (Raible et al., 2006) independently analyzed the genome of the echinoid *Strongylocentrotus purpuratus* and found six opsins from at least three pan-bilaterian families (r-opsin, c-opsin, G_o-opsin) that were most strongly expressed in the tube feet and the globiferous and tridentate pedicellariae (expression in the

endoskeleton was not measured). While other recent work has found some remarkable adaptations in the endoskeleton of echinoderms, including polarizing filters, migrating pigments and arrays of microscopic lenses (Hendler, 1984; Johnsen, 1994; Aizenberg et al., 2001), no regional specialization akin to cephalization has been found, leaving open the question of the neurological and structural bases of these photobehaviors.

Woodley (Woodley, 1982) attempted to reconcile the ability of the tropical urchin *Diadema antillarum* to move towards small, dark objects with its apparent lack of an image-forming eye by suggesting that the entire animal functions as a compound eye, with the spines screening off-axis light, much like screening pigments optically separate ommatidia in insect eyes (Land and Nilsson, 2002). Blevins and Johnsen tested this hypothesis using echinoids of the genus *Echinometra* and found that their visual resolution was on the order of that predicted by the spacing of their spines (~ 30 deg.) (Blevins and Johnsen, 2004).

This paper examines the visual resolution of *S. purpuratus*. Like *Echinometra*, it exhibits shelter-seeking behavior and is known to have a photosensitive test. However, the angular density of its spines is roughly double–triple that of *Echinometra*. We therefore performed similar experiments to those described by Blevins and Johnsen (Blevins and Johnsen, 2004) to determine whether *S. purpuratus* had correspondingly higher visual resolution.

MATERIALS AND METHODS

Specimen collection and care

Twenty adult specimens of *Strongylocentrotus purpuratus* Stimpson 1857 were collected at Corona del Mar State Beach (33°35'N 117°52'W; Corona del Mar, CA, USA) by Charles Halloran, Inc. or obtained from Pat Leary at California Institute of Technology (Pasadena, CA, USA). They were kept in a covered aquarium at 15°C, under constant light, at a salinity of 30–35 p.p.t. While a 12h:12h light:dark cycle would have been preferable, captive *S. purpuratus* will often spawn in darkness, which fouls the water and can lead to significant mortality and morbidity. Because we found that even moderately unhealthy urchins did not move in the testing arena, they were kept under constant light and tested as soon as possible after collection (within two weeks).

Experimental apparatus

The experimental arena was similar to that used by Blevins and Johnsen (Blevins and Johnsen, 2004) and consisted of a covered fiberglass tank (1.2 m diameter) with a glass bottom (Fig. 1A). The

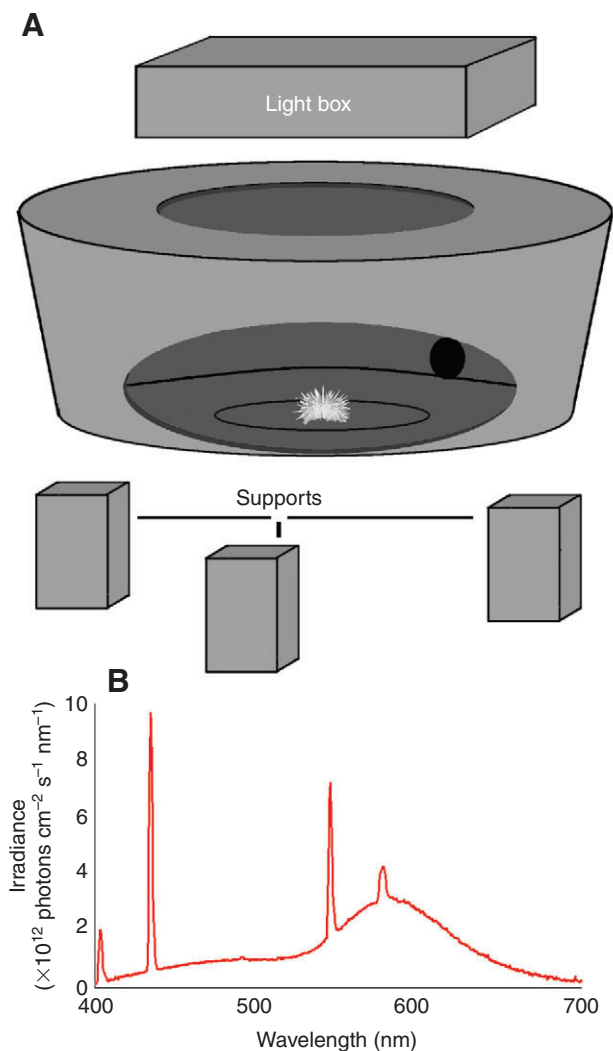


Fig. 1. (A) Diagram of testing arena. The circular black target can be seen on the back of the inside of the tank. The circle around the urchin denotes the distance the urchins must move before their bearing is recorded (16 cm). The elliptical hole in the side of the tank serves only to show the inside and is not found on the actual tank. (B) Downwelling spectral irradiance at the center of the arena.

covering of the tank had a small opening on one side and a large central circular opening that measured 0.4 m in diameter. A diffuse fluorescent light source was placed above the circular opening, resulting in a downwelling irradiance (integrated from 400–700 nm) at the arena floor of 4×10^{14} photons $\text{cm}^{-2} \text{s}^{-1}$ [measured using an Ocean Optics USB2000 Spectroradiometer fitted with a CC3 cosine corrector, Dunedin, FL, USA; Fig. 1B). The tank was mounted on four cement blocks, and white cloth was placed directly under the glass bottom to allow unobtrusive observation of the urchins' shadows from below. The cloth was marked with a 32 cm diameter circle centered at the middle of the arena and divided into 15 deg. increments.

A black circular plastic target (5% diffuse reflectance, 1% specular reflectance) with a diameter of either 6 cm or 9 cm was attached to the wall of the tank. At this distance from the center of the arena (0.52 m), the diameters of the two targets subtended angles of ~6.5 deg. and 10 deg. (and their areas subtended solid angles of 0.01 sr and 0.024 sr). The reflectance of the arena wall was ~50% from 450–500 nm (the likely predominant wavelengths for echinoid photosensitivity), giving the target a Weber contrast of ~0.9.

Experimental procedure

On each day of trials, the arena was filled with artificial seawater of the same temperature and salinity as that in the holding aquarium. Each urchin was tested four times in a row, with the target placed successively at 0 deg., 90 deg., 180 deg. and 270 deg. (relative to magnetic east). The four different target positions allowed us to control for any spurious orientation to other features of the arena, room or external environment. The urchin was first placed in the center of the tank. Then the arena door was closed, the lights were turned on and the movement of the urchin was observed from below. The urchins generally began moving within 60 s, almost always in a straight line. Once the urchin moved 16 cm from the center, its bearing was recorded to the nearest 15 deg. Animals were stopped at 16 cm so that the angular size of the target (as viewed by the urchin) would not change significantly and potentially affect the results. The maximum angular diameters of the 6.5 deg. and 10 deg. targets at 16 cm from the center occurred when the animal moved directly towards the target and were 9.5 deg. and 14 deg., respectively. The minimum angular diameters of the targets at 16 cm from the center occurred when the animal moved directly away the target and were 5.0 deg. and 7.5 deg. Given that the animals moved in a straight line, the choice was almost certainly made based on the perception of angular size from the center of the arena. After the trial, the light was then turned off, the urchin was returned to a holding tank and the arena was scrubbed to reduce the potential for trail following. Then the urchin was returned to the center of the arena for the additional three trials (with randomly ordered target bearings). After the four trials, the mean absolute bearing (\vec{V}_{abs}) for a given urchin was calculated using:

$$\vec{V}_{\text{abs}} = (V_x, V_y) = \frac{1}{4} \left(\sum_{i=1}^4 \cos \phi_i, \sum_{i=1}^4 \sin \phi_i \right), \quad (1)$$

where ϕ_i was the bearing of the urchin in the i th trial (relative to magnetic east) (Fig. 2A). The average bearing vector corrected ($\vec{V}_{\text{corrected}}$) for the moving position of the target (referred to hereafter as the target-normalized bearing) is:

$$\vec{V}_{\text{corrected}} = (V_x, V_y) = \frac{1}{4} \left(\sum_{i=1}^4 \cos(\phi_i - \omega_i), \sum_{i=1}^4 \sin(\phi_i - \omega_i) \right), \quad (2)$$

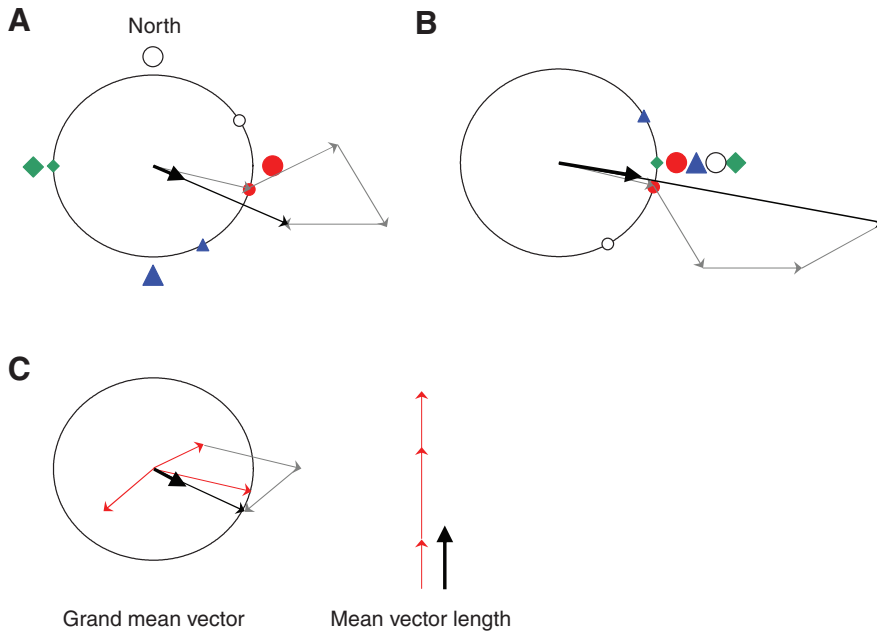


Fig. 2. Description of analysis. (A) Calculation of mean vector for the four absolute bearings of one urchin (symbols on circle) where the target is placed at the four compass points (matching larger symbols outside circle). The mean vector (bold short arrow) is one-quarter of the vector sum of the four bearing vectors (individual vectors in gray, sum vector in black, calculated using Eqn 1). (B) Calculation of the mean vector for target-normalized bearings (using Eqn 2). (C) Explanation of difference between the calculation of grand mean vector and that of average vector length for three sample urchins. The grand mean vector was calculated for both absolute and target-normalized vectors but in this example is done for target-normalized bearings. Each red arrow is the mean target-normalized vector (calculated using Eqn 2 based on four trials) for one urchin. The grand mean vector is one-third of the vector sum of the three mean vectors (calculated using Eqn 5). The average vector length is one-third of the simple sum of the lengths of the three mean vectors. The surrounding black circles in all three panels denote a vector length (R) of one.

where ω_i was the bearing of the target (0 deg., 90 deg., 180 deg. or 270 deg.) in the i th trial (Fig. 2B). As mentioned above, these corrected bearings control for orientation to other features in the environment. If the urchins are detecting the target and moving at some set angle relative to it, the corrected bearing vectors will remain consistent while the absolute bearings will be scattered.

For both the absolute and target-normalized bearings, the length of \vec{V} (generally referred to as ‘ R ’ in circular statistics) is given by:

$$R = |\vec{V}| = \sqrt{V_x^2 + V_y^2}. \quad (3)$$

In this case, R is a measure of the consistency of the headings of a given urchin over its four trials, with $R=1$ implying that the animal moved in the same direction (either absolute or relative to the target) all four times. Monte Carlo methods (see below) show that, for the four trials, the value of R expected by chance has a wide distribution centered around 0.45 (i.e. the average length of the vector sum of four randomly oriented unit vectors is $4 \times 0.45 = 1.8$).

The average angle over the four trials (θ) is given by:

$$\theta = \tan^{-1} \left(\frac{V_y}{V_x} \right) (+180 \text{ deg. if } V_x < 0). \quad (4)$$

The grand mean vector (\vec{V}_{GM}) for all of the 20 trials (which was used for testing for significant orientation of the urchins) was calculated for both absolute and target-normalized bearings using:

$$\vec{V}_{GM} = \frac{1}{20} \left(\sum_{j=1}^{20} \cos \theta_j, \sum_{j=1}^{20} \sin \theta_j \right), \quad (5)$$

where θ_j is the average bearing of the j th urchin calculated using Eqn 4. The length and angle of the grand mean vector are calculated using equations analogous to Eqns 3 and 4. It is important to note that the length of the grand mean vector is not the same as the average of the lengths of the vectors for each animal, because it is a vector sum and thus takes the directions of each vector into account. For example, if six urchins were tested and three always went directly towards the target (in all four trials) and three always went directly away from it, the length of the grand mean vector would be zero, but the average of the lengths of the vectors for the urchins

would be 1, i.e. even though the group as a whole did not choose one direction relative to the target, they obviously responded to it. This is analogous to a group of people each using their own compass to go a different direction.

Data analysis

The collection of bivariate data (R_j, θ_j) was tested for significant orientation using either Hotelling’s test or, if either of the x or y components of the bearings were not normally distributed, a non-parametric version of Hotelling’s test developed by Moore (Moore, 1980) (but see Batschelet, 1981). Tests for significant unimodal and axial orientation were performed for both absolute bearings and target-normalized bearings.

Preliminary examination of the data suggested that the mean vectors for the target-normalized bearings for the 10 deg. target (calculated using Eqn 3) were unusually long. This was tested in two ways. First, cumulative histograms of the mean vector lengths of absolute and target-normalized bearings were compared with that expected due to random chance using the Kolmogorov–Smirnov test. In addition, because it is extremely difficult to accurately determine the Kolmogorov–Smirnov distribution for very low P -values, Monte Carlo methods were also used to test whether the average length of the 20 mean vectors was non-random. Ten billion (10^{10}) runs of 20 urchins, each run four times with random bearings, were generated. The average of the mean vector lengths was calculated for each run (note that this is NOT the length of the grand average vector):

$$\bar{R} = \frac{1}{20} \sum_{i=1}^{20} R_i. \quad (6)$$

A histogram of 10^{10} \bar{R} ’s was generated and compared with the experimental value. The Monte Carlo simulation was programmed using Matlab (Mathworks, Natick, MA, USA).

RESULTS

Bearings of urchins using 6.5 deg. target

The absolute bearings, uncorrected for the position of the target, showed no significant unimodal or axial orientation (Fig. 3A, Table 1). The target-normalized bearings also showed no significant

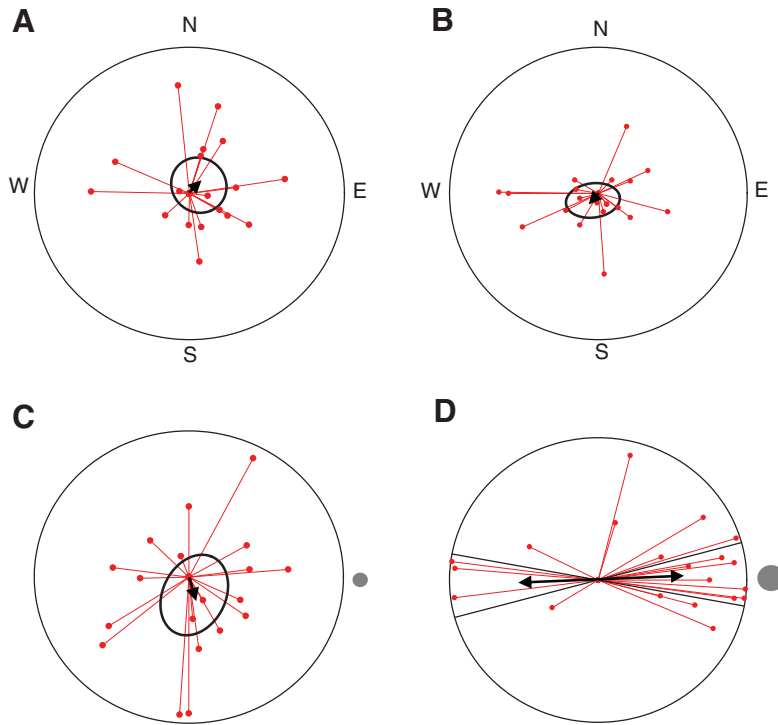


Fig. 3. (A) The absolute average bearings for each echinoid tested against the 6.5 deg. target (averaged over their four trials) (N, E, W and S are geomagnetic compass points). (B) The absolute average bearings for each echinoid tested against the 10 deg. target. (C) The average bearings relative to the position of the 6.5 deg. target (shown to scale in gray at the right of the graph). (D) The average bearings relative to the position of the 10 deg. target (shown to scale in gray at the right of the graph). The red lines show the length and direction of the average bearing for the four trials with one echinoid. Red lines that reach the outer circle imply that the echinoid went the same direction in all four trials (either un-normalized or relative to the target). The bold black lines show the average vector sum of the 20 average bearings, also known as the grand mean vector. Only the grand mean vector for unimodal orientation is shown in A, B and C, and only the grand mean vector for axial orientation is shown in D. The black ellipses in A–C are 95% confidence ellipses for the magnitude and direction of the grand mean vector (i.e. the endpoint of the bold, black arrow has a 95% confidence of lying within the ellipse). The boundaries of the 95% confidence interval for the mean angle of the grand mean vector are also shown in black in D (a confidence ellipse cannot be used because the data is not normal). The large surrounding black circles in all four panels denote a vector length (R) of one.

unimodal or axial orientation (Fig. 3C; Table 1). The distribution of the lengths of the absolute vectors relative to that expected by chance was borderline significant ($P=0.044$, Kolmogorov–Smirnov test). The distribution of the lengths of the target-normalized vectors was not significantly different from chance (Table 1).

Bearings of urchins using 10 deg. target

The absolute bearings showed no significant unimodal or axial orientation (Fig. 3B, Table 1). Analyzed unimodally, the target-normalized bearings also showed no significant orientation. However, the target-normalized bearings were axially oriented with high significance (mean axis from -1 to 179 deg.; 95% confidence interval ± 12 deg.; $P<0.00025$), with 10 out of the 20 urchins choosing

an average bearing within 10 deg. of either the target or its opposite direction (Fig. 3D, Table 1). The distribution of the lengths of the target-normalized vectors was significantly different from chance ($P\leq 0.001$, Kolmogorov–Smirnov test), with an average vector length of 0.77 ± 0.05 – far higher than the expected average of 0.45 ($P<10^{-10}$, Monte Carlo simulation). The distribution of the lengths of the absolute vectors was also significantly different from that expected by chance ($P<0.001$, Kolmogorov–Smirnov Test), with an average vector length of 0.29 ± 0.04 – lower than the expected average of 0.45 ($P<0.001$, Monte Carlo simulation). It is important to note that, because the target is moved to four different positions, an urchin that follows it will have a long target-normalized bearing vector and a short absolute bearing vector.

Table 1. Absolute and target-normalized bearings of urchins

Bearings	θ (grand mean, deg.)	95% confidence	R (grand mean)	P -value (orientation)	R (average length)	P -value (R lengths)
6.5 deg. target ($N=19$)						
Absolute						
Unimodal	-118	–	0.083	n.s.*	0.36	0.044 [‡]
Axial	175–355	–	0.016	n.s.*	–	–
Target-normalized						
Unimodal	74	–	0.13	n.s.*	0.51	n.s. [‡]
Axial	110–290	–	0.090	n.s.*	–	–
10 deg. target ($N=20$)						
Absolute						
Unimodal	-140	–	0.060	n.s.*	0.29	<0.001 [‡]
Axial	80–260	–	0.096	n.s.*	–	–
Target-normalized						
Unimodal	-15	–	0.34	n.s. [†]	0.77	<10 ^{-10§}
Axial	-2.3–178	± 13 deg.	0.55	<0.001 [†]	–	–

*Hotelling’s one-sample test.

[†]Moore’s non-parametric test for bivariate data.

[‡]Kolmogorov–Smirnov test.

[§]Monte Carlo simulation.

DISCUSSION

Two aspects of the results strongly suggest that *S. purpuratus* was able to detect a 10 deg. diameter target whose solid angle was less than 0.2% of the total visual field. First, as a population, the animals were strongly axially oriented, with half of them orienting to within 10 deg. of the target center or its opposite bearing. Second, the orientation of individual animals was remarkably strong, with almost all of the urchins moving consistently either towards or away from the target as it was placed at four different bearings.

The bimodal nature of the response (and its consistency over four trials for a given animal) suggests that it is unlikely to be a simple phototaxis. Also, measurements using the spectroradiometer described above showed that the horizontal irradiance on the side of the urchin facing the dark target is only 1% less than that on the side of the urchin facing away from the target – less than the ~5% azimuthal variation of horizontal irradiances in an empty arena measured over the eight compass points. Therefore, any response based on only the irradiance at the surface of the urchin would have been even more strongly affected by the slight (but larger) azimuthal variation in the arena irradiance and lead to significant orientation of the absolute bearings. Also, the variations in horizontal irradiance in even the most uniform underwater environment are far higher than 1–5% and also vary continually, suggesting that movements based on irradiance changes of a few percent would be maladaptive.

With the exception of one borderline significant result (that either Bonferroni correction or control of false discovery rate eliminates) there was no evidence that the urchins responded to the 6.5 deg. target, suggesting that the 10 deg. target is close to the lower threshold of what can be detected by *S. purpuratus*. However, it is

important to note that the exact spatial resolution of *S. purpuratus* cannot be determined from the results of this study because a single object on an empty background can be detected by visual systems with lower resolution than the object's size. However, calculations by Blevins and Johnsen (Blevins and Johnsen, 2004) showed that objects significantly smaller than the resolution limit of a viewer can only be detected if the viewer is sensitive to very small changes in brightness over graded boundaries (luminous objects on a black background such as stars are an exception because their contrast is essentially infinite). Some aquatic vertebrates can detect radiance differences of ~1–2% under ideal conditions (Douglas and Hawryshyn, 1990). However, the regions with the differing radiances must be adjacent and separated by a sharp border (Land and Nilsson, 2002). Gradual changes in radiance are far more difficult to detect. Thus, the spatial resolution of *S. purpuratus* is likely to be at least 10 deg. It is, of course, possible that the urchins possess higher acuity but were not motivated to move towards or away from the smaller target (perhaps not perceiving it as large enough to be a threat or useful shelter). This classical issue of motivation *versus* perception is difficult to address in any experimental system. At present though, there is no proposed optical mechanism for higher acuity.

This resolution is consistent with the hypothesis that spatial vision in echinoids is mediated by screening of off-axis light by the spines, much like photostable pigments screen off-axis light in compound eyes. In the regions of the test of *S. purpuratus* that faced horizontally, spines were spaced by about 4 deg. in the interambulacrum and 5.5 deg. in the ambulacrum (Fig. 4, see caption for details of measurements). Given that the test is convex and that the spines are more or less perpendicularly to its surface, on average

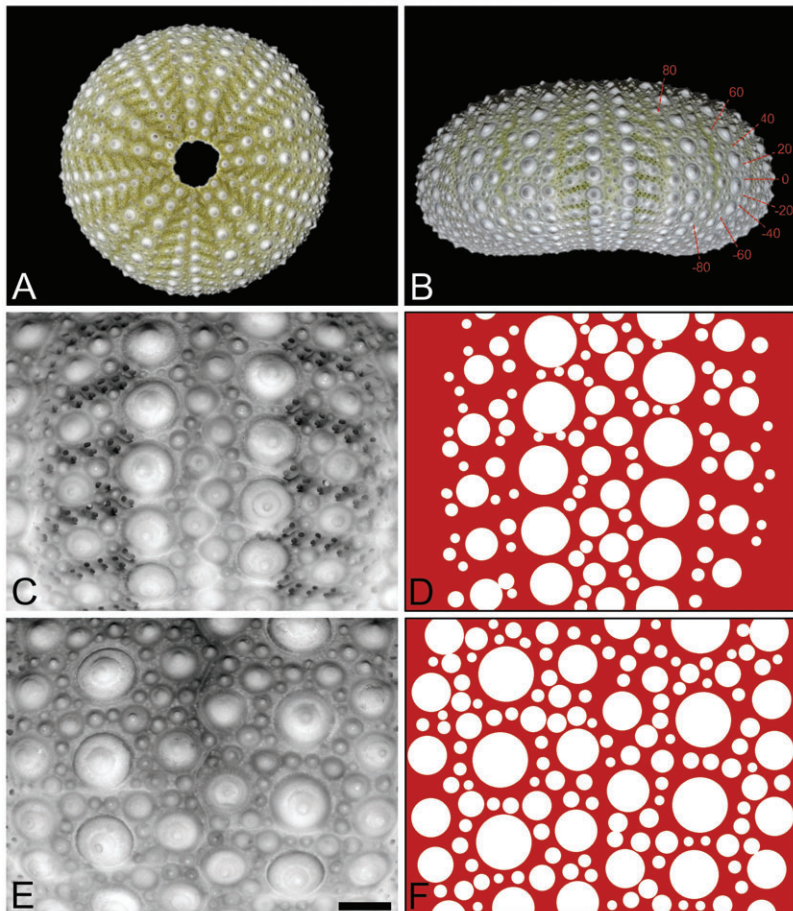


Fig. 4. Denuded test of *Strongylocentrotus purpuratus* showing spine density. (A) Plan view. (B) Profile view showing angles of vectors normal to the surface. (C) Portion of ambulacrum (region with tube feet). (D) Diagram of ambulacrum region shown in C. (E) Portion of interambulacrum region shown in E. Regions shown in C and E are those that face horizontally, because those are the most likely to be involved in detecting targets on the horizon. Red portions of D and F indicate regions of the test that are not covered by the base of a spine and thus most likely to be photosensitive. Scale bar is 5 deg. in the horizontal direction and 15 deg. in the vertical direction (the vertical curvature is higher than the horizontal curvature in this region of the test). The horizontal spine densities quoted in the text were calculated by drawing 17 evenly spaced horizontal lines across both the ambulacrum and interambulacrum and counting the number of intersections with spines.

any given photosensitive region of the horizontally facing portion of the test and pedicellariae would have its horizontal field of view restricted to about 4–5.5 deg. [see Blevins and Johnsen for figures and further details (Blevins and Johnsen, 2004)]. From signal theory, detail can be resolved over angles that are double the angular resolution of the detector (Land and Nilsson, 2002), so, based on spine density, *S. purpuratus* is predicted to have a spatial resolution of 8–11 deg., which approximates the experimental results. The urchins *Echinometra lucunter* and *Echinometra viridis* moved towards 33 deg. targets but not towards 26 deg. or 16 deg. targets (Blevins and Johnsen, 2004). Similar measurements on this genus show that the horizontal density of the spines in the horizontal-facing region of their test is about 12.5 deg. (interambulacrum) and 9.5 deg. (ambulacrum), predicting a horizontal acuity between 19 deg. and 25 deg. in the horizontal direction [slightly higher than the global spine density given in Blevins and Johnsen (Blevins and Johnsen, 2004), due to regional variation]. This is somewhat better than the behavioral results show, suggesting that other factors, ranging from motivation to other morphological features of the test and pedicellariae, also play a role. Another issue is that the spacing of the spines is highly variable, depending on the exact region of the test, so exact predictions are problematic. Unfortunately, because clipping or removing substantial numbers of spines drastically affects both the locomotion and the health (and thus motivation) of the urchins, a more direct test of the hypothesis that the spine density mediates spatial vision is not possible. However, morphological studies of the tests and pedicellariae of echinoids have found no evidence for the screening of off-axis light (reviewed by Yoshida et al., 1983), leaving the spines as the most likely candidate to mediate this level of visual acuity.

The ecological function of movement towards and away from small dark objects in *S. purpuratus* is unknown, but is likely to be related to shelter seeking and predator avoidance, respectively. *Strongylocentrotus purpuratus*, found on the west coast of North America, mostly resides in shallow, wave-swept habitats, foraging on drifting algal detritus or grazing on attached plants (Workman, 1999; Tegner, 2001). When these food items become scarce, the urchins switch to active foraging (Tegner, 2001), which would presumably be enhanced by even moderate visual acuity. Additionally, *S. purpuratus*, like *Echinometra*, is often found in small, dark boreholes – presumably to protect them from wave forces and predation – that they would need to locate after foraging (Verling et al., 2004). While intertidal populations move very little, and can actually become trapped for life in their boreholes, subtidal populations (from which the experimental animals were drawn) may migrate over moderate distances for spawning or foraging (reviewed by Workman, 1999). Spatial vision may also facilitate the aggregation that can precede mass spawning. Finally, while visual detection offers no real protection against their primary predator, sea otters, it may allow *S. purpuratus* to successfully retreat from its slower predators, such as the sea stars *Pycnopodia helianthoides* and *Pisaster ochraceus*.

We originally expected that the urchins would move consistently towards the target, based on the shade-seeking behavior found in certain other echinoderms (e.g. Johnsen and Kier, 1999; Aizenberg et al., 2001; Adams, 2001). In particular, the congeneric species *Strongylocentrotus droebachiensis* seeks shade, although only in the presence of UV radiation (Adams, 2001). However, one quarter of the specimens of *S. purpuratus* moved consistently and directly away from the target. We speculate that the two behaviors represent two different motivational states related to opposing interpretations of the target, mostly likely to be shelter versus predator. Distinguishing a predator from a harmless or beneficial target (e.g.

shelter, conspecific) is a difficult problem for species with low-resolution vision and is likely to be particularly problematic for urchins given their low visual acuity and slow movements. Some species solve this problem using simple rules. For example, the fiddler crab *Uca pugilator*, which has a resolution of 1–5 deg., sorts predators from conspecifics entirely by their position relative to the horizon, with anything above the horizon being considered a (presumably avian) predator (Land and Layne, 1995; Zeil and Hemmi, 2005). The snapping shrimp *Synalpheus demani* apparently sorts shade from predator by angular size, approaching 90 deg. or larger targets and fleeing from 30 deg. targets (Huang et al., 2005). The ophiuroid *Ophiocoma wendtii* responds in a similar manner, fleeing from shadows cast on it and moving towards dark regions on the horizon (Aizenberg et al., 2001). Future studies will examine whether the target's position, shape or size affects the polarity of the urchins' responses.

Finally, it is possible that the polarity of the response is cyclical, as was found in the amphipod *Talitrus saltator*, which moves alternately towards or away from small dark object depending on time of day, with a pattern that matched its natural migrations up and down the beach (Scapini, 1997). While the tests in the present study were all performed within a relatively narrow time window during the middle of the day, it is nevertheless possible that individuals were at different points in some endogenous rhythm that affected behavior.

In conclusion, the spatial visual resolution in *S. purpuratus* appears to be predicted by the density of its spines, lending further support to the hypothesis that at least some echinoids operate as large compound eyes. The resolution of the system is far lower than that of vertebrate camera eyes but roughly equal to that of the chambered *Nautilus* and the horseshoe crabs, suggesting that the visual behavior of echinoids may be more complex than previously appreciated.

ACKNOWLEDGEMENTS

We thank Drs David McClay and Gregory Wray for the use of their urchins and Drs Alison Sweeney, Eric Warrant and Tamara Frank for comments on earlier drafts. S.J. was supported in part by a grant from the National Science Foundation (IOB-0444674).

REFERENCES

- Adams, N. (2001). UV radiation evokes negative phototaxis and covering behavior in the sea urchin *Strongylocentrotus droebachiensis*. *Mar. Ecol. Prog. Ser.* **213**, 87–95.
- Aizenberg, J., Tkachenko, A., Weiner, S., Addadi, L. and Hendler, G. (2001). Calcitic microlenses as part of the photoreceptor system in brittlestars. *Nature* **412**, 819–822.
- Batschelet, E. (1981). *Circular Statistics in Biology*. New York: Academic Press.
- Blevins, E. and Johnsen, S. (2004). Spatial vision in the echinoid genus *Echinometra*. *J. Exp. Biol.* **207**, 4249–4253.
- Burke, R. D., Angerer, L. M., Elphick, M. R., Humphrey, G. W., Yaguchi, S., Kiyama, T., Liang, S., Mu, X., Agca, C., Klein, W. H. et al. (2006). A genomic view of the sea urchin nervous system. *Dev. Biol.* **300**, 434–460.
- Hendler, G. (1984). Brittlestar color change and phototaxis (Ophiocomidae). *PSZNI Mar. Ecol.* **5**, 9–27.
- Huang, H.-D., Rittschoff, D. and Jeng, M.-S. (2005). Visual orientation of the symbiotic snapping shrimp *Synalpheus demani*. *J. Exp. Mar. Biol. Ecol.* **326**, 56–66.
- Johnsen, S. (1994). Extraocular sensitivity to polarized light in an echinoderm. *J. Exp. Biol.* **195**, 281–291.
- Johnsen, S. and Kier, W. M. (1999). Shade-seeking behavior under polarized light by the brittlestar *Ophioderma brevispinum*. *J. Mar. Biol. Assoc. UK* **79**, 761–763.
- Land, M. F. and Layne, J. (1995). The visual control of behaviour in fiddler crabs: I. Resolution, thresholds and the role of the horizon. *J. Comp. Physiol. A* **177**, 81–90.
- Land, M. F. and Nilsson, D.-E. (2002). *Animal Eyes*. Oxford University Press, New York.
- Millot, N. (1954). Sensitivity to light and the reactions to changes in light intensity of the echinoid *Diadema antillarum Philippi*. *Phil. Trans. Roy. Soc. B.* **238**, 187–220.
- Millot, N. (1955). The covering reaction in a tropical sea urchin. *Nature* **175**, 561.
- Millot, N. and Yoshida, M. (1960). The shadow reaction of *Diadema antillarum*: the spine response and its relation to the stimulus. *J. Exp. Biol.* **37**, 363–375.
- Moore, A. and Cobb, J. L. S. (1985). Neurophysiological studies on photic responses in *Ophiura ophiura*. *Comp. Biochem. Physiol.* **80A**, 11–16.
- Moore, B. R. (1980). A modification of the Rayleigh test for vector data. *Biometrika* **67**, 175–180.

- Raible, F., Tessmar-Raible, K., Arboleda, E., Kaller, T., Bork, P., Arendt, D. and Arnone, M.** (2006). Opsins and clusters of sensory G-protein coupled receptors in the sea urchin genome. *Dev. Biol.* **300**, 461-475.
- Scapini, F.** (1997). Variation in scototaxis and orientation adaptation of *Talitrus saltator* populations subjected to different ecological constraints. *Estuar. Coast. Shelf Sci.* **44**, 139-146.
- Scheibling, R. E.** (1980). Homing movements of *Oreaster reticulatus* when experimentally translocated from a sand patch habitat. *Mar. Behav. Physiol.* **7**, 213-223.
- Tegner, M. J.** (2001). The ecology of *Strongylocentrotus franciscanus* and *Strongylocentrotus purpuratus*. *Edible Sea Urchins: Biology and Ecology*. New York: Elsevier.
- Thornton, I. W. B.** (1956). Diurnal migrations of the echinoid *Diadema setosum*. *Brit. J. Anim. Behav.* **4**, 143-146.
- Verling, E., Crook, A. C. and Barnes, D. K. A.** (2004). The dynamics of covering behaviour in dominant echinoid populations from American and European west coasts. *Mar. Ecol.* **25**, 191-206.
- Woodley, J. D.** (1982). Photosensitivity in *Diadema antillarum*: does it show scototaxis? In *The International Echinoderm Conference, Tampa Bay* (ed. J. M. Lawrence), pp. 61. Rotterdam: A. A. Balkema.
- Workman G.** (1999). *A Review of the Biology and Fisheries for Purple Sea Urchin (Strongylocentrotus purpuratus, Stimpson, 1957) and Discussion of the Assessment Needs of a Proposed Fishery*. Canadian stock assessment secretariat research document 99/163. Fisheries and Oceans Canada, Ottawa.
- Yoshida, M.** (1966). Photosensitivity. In *Physiology of Echinodermata* (ed. R. A. Booloottian), pp. 435-464. New York: John Wiley and Sons.
- Yoshida, M.** (1979). Extraocular photoreception. In *Handbook of Sensory Physiology* vol. 7/6A (ed. H. Autrum), pp. 581-640. New York: Springer-Verlag.
- Yoshida, M., Takasu, N. and Tamotsu, S.** (1983). Photoreception in echinoderms. In *Photoreception and Vision in Invertebrates* (ed. M. A. Ali), pp. 743-772. New York: Plenum Press.
- Zeil, J. and Hemmi, J. M.** (2005). The visual ecology of fiddler crabs. *J. Comp. Physiol. A* **192**, 1-25.